Research Square

Preprints are preliminary reports that have not undergone peer review.
They should not be considered conclusive, used to inform clinical practice,
or referenced by the media as validated information.

Effect of lateral mechanical smoke exhaust on smoke backflow behavior and temperature profile in a mountain tunnel: A numerical investigation and analysis

Mintao Jia
Central South University
Shaoxuan Wang
Hebei University of Engineering
Li Chen
Hebei University of Engineering
Xudui Liu
Hebei University of Engineering
Yupeng Hao
Hebei University of Engineering
Mingxuan Yang
Hebei University of Engineering
Jiaxian Cheng
Hebei University of Engineering
Wenxin Qiu
Hebei University of Engineering
Zhisheng Li
lzsfire@163.com

Hebei University of Engineering

Article

Keywords: Mechanical smoke exhaust, Lateral opening shaft, Smoke movement, Smoke back-layering length, Temperature profile

Posted Date: July 6th, 2026

DOI: https://doi.org/10.21203/rs.3.rs-10128901/v1

License: This work is licensed under a Creative Commons Attribution 4.0 International License.
Read Full License

Additional Declarations: No competing interests reported.

Version of Record: A version of this preprint was published at Scientific Reports on September 21st, 2026. See the published version at https://doi.org/10.1038/s41598-026-72721-6.

Effect of lateral mechanical smoke exhaust on smoke backflow behavior and temperature profile in a mountain tunnel: A numerical investigation and analysis

Mintao Jia[a,b,c], Shaoxuan Wang [d], Li Chen[d**], Xudui Liu[d], Yupeng Hao[d], Mingxuan Yang[d], Jiaxian Cheng[d], Wenxin Qiu[d], Zhisheng Li[c,d*]

[a] School of Resources and Safety Engineering, Central South University, Changsha, 410083, China

[b] Sinosteel Maanshan General Institute of Mining Research Co., Ltd., Maanshan 243000, China

[c] State key Laboratory of Metal Mining Safety and Disaster Prevention and Control, Maanshan 243000, China

[d] School of Mining and Geomatics Engineering, Hebei University of Engineering, Handan 056038, China

*Co-corresponding author information:

Name: Zhisheng Li, and Li Chen
Address: School of Mining and Geomatics Engineering, Hebei University of Engineering, Handan, 056038, China
Email: lzsfire@163.com , and chenli1981@hebeu.edu.cn

Abstract

This study involved a series of numerical simulations to examine smoke movement and temperature profiles, with variations in heat release rate and smoke exhaust velocity. A considerable disparity in smoke migration behavior is evident when the mechanical smoke exhaust methods of the ceiling opening shaft and the lateral opening shaft are compared. The asymmetric distribution of the flow field in the lateral opening mechanical smoke exhaust mode was identified and elucidated. A quantitative analysis and numerical observation were conducted to examine the longitudinal attenuation of smoke temperature upstream and the smoke back-layering length in a tunnel with a lateral opening shaft. Consequently, two empirical models were developed to forecast the longitudinal temperature decay and the smoke back-layering length, respectively. This work serves as a significant reference for the design of ventilation and smoke extraction systems in mountain tunnels featuring lateral open shafts.

Keywords: Mechanical smoke exhaust; Lateral opening shaft; Smoke movement; Smoke back-layering length; Temperature profile

1. Introduction

In recent years, a large amount of underground space has been used in the fields of coal mine industrial production, transportation and commerce. As a special underground space, tunnel has brought great convenience to human production and life. Nevertheless, previous reports have documented the frequent occurrence of fire incidents in tunnels over the past few decades (Beard, 2009; Ingason H, 2015; Ren et

al., 2019; Zhu et al., 2022b). The safety of personnel and fire rescue is considered to be a significant hazard due to the large quantity of high-temperature, toxic, and harmful gases that are produced during tunnel fires. Occasionally, the design and construction of inclined shafts are challenging due to the constraints of existing structures or geological conditions. For instance, the general Mine tunnel, Maluanshan road tunnel, and (Li et al., 2025a; Li et al., 2021b; Li et al., 2022) Qinling extra-long road tunnel (Wang et al., 2021) is a viable option for the design of a cross passage that connects the shaft and the primary tunnel in this scenario. Consequently, it is imperative to examine the behavior of smoke movement in a tunnel with a lateral open shaft.

In the past decade, there has been a significant amount of research conducted on the temperature profile and the smoke back-layering decay, which are critical parameters that reflect the behavior of smoke movement and are used to assess the fire hazard. The longitudinal temperature distribution and maximal excess temperature were thoroughly investigated in relation to the temperature profile beneath the ceiling. A traditional tunnel's maximal excess temperature was investigated through theoretical analysis and experiments. As a result, Kurioka (Kurioka et al., 2003) and Li (Li et al., 2011) developed the classical models for predicting the maximal excess temperature. The smoke spread process continuously entrains the surrounding air and encounters the surrounding wall, resulting in heat loss. Consequently, it is the reduction of the temperature distribution. In accordance with prior studies (Gong et al., 2016; Hu et al., 2004; Ji et al., 2012), the exponential function is an effective representation of

longitudinal temperature decay. The back-layering is typically restricted to a specific distance where the smoke front reaches a halt when the buoyancy-driven plume extends along the ceiling and interacts with the longitudinal wind. At the same time, the smoke strata accumulated beneath the ceiling. A criterion for evaluating the halting countercurrent of smoke is that the dynamic pressure generated by the longitudinal wind is equivalent to the static pressure of the smoke layer (Chow et al., 2015; Hu et al., 2008). Another model was obtained by Li et al.(Li et al., 2010) by performing dimensional analysis.

The smoke movement behavior during the activation of the shaft centralized smoke exhaust system is subtly distinct from that of conventional single-tube tunnel fires. Hu et al. (Hu et al., 2014) proposed an induced longitudinal velocity to quantify the impact of the shaft-centralized smoke exhaust on the smoke movement. The modified correlations were obtained by investigating the temperature distribution and smoke-layering length (Chen et al., 2013; Chen et al., 2015), where the fire source is situated immediately beneath the shaft. Additionally, Tang et al. conducted experimental and theoretical investigations of the maximum excess temperature (Tang et al., 2017b), longitudinal temperature decay (Tang et al., 2018a), and air entrainment (Tang et al., 2018b), where the fire source is located on the upstream side of the shaft. Wang et al. (Wang et al., 2018) postulated a predicted correlation of smoke back-layering length in the case of a fire source situated on the downstream side of the shaft. Wan et al. (Wan et al., 2019) conducted a numerical simulation to investigate the smoke back-layering length in the context of the coupling effect of

tunnel slope and natural smoke emission in the shaft. The concept of tunnel inlet wind speed was introduced to quantify the impact of the shaft and slope on smoke back-layering length.

Nevertheless, it is important to note that the majority of the aforementioned studies concentrated on the impact of the longitudinal ventilation system and ceiling smoke extraction system on smoke movement. The primary focus of these investigations was a road tunnel. In an effort to enhance the quality of intercity transportation, expansive mountain tunnels have been constructed in recent years. The asymmetry of smoke flow behavior in the tunnel is frequently the result of the vertical shaft being laterally connected to the main tunnel through the channel (Li et al., 2025a; Li et al., 2021b; Li et al., 2022; Wang et al., 2021; Zhang, 2025). Additionally, despite the fact that the investigation of smoke plug-holing behavior (Zhu et al., 2022a) and carbon dioxide concentration distribution (Xu et al., 2018) was conducted in a tunnel with a lateral smoke exhaust port, there are still some knowledge gaps regarding the distribution of temperature and the spread of smoke in a tunnel with a lateral open shaft. Given this, a series of numerical simulations was performed to examine the impact of the mechanical exhaust velocity of the lateral opening shaft on the maximal excess temperature, longitudinal temperature distribution, and smoke back-layering length. The smoke countercurrent length change law, in order to offer data support and guidance for the prevention and control of fires in tunnels. The following are the contributions of this work: 1) demonstrating the distinction in smoke movement behavior between mechanical smoke exhaust in a lateral open shaft and concentrated

smoke exhaust in the ceiling. 2) Developing the model to forecast the longitudinal temperature decay and smoke back-layering length under the lateral open shaft smoke exhaust.

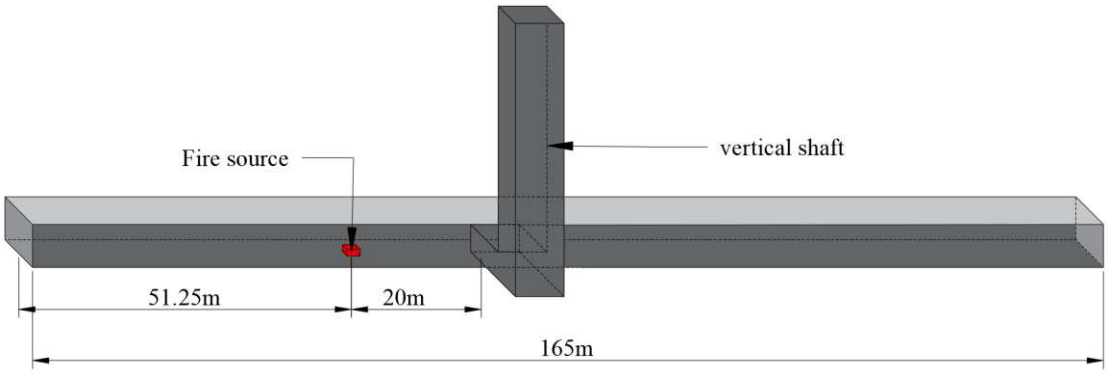
2. Numerical Modeling

To investigate the impact of the mechanical smoke exhaust system on the characteristics of fire smoke propagation in a tunnel featuring a lateral opening shaft, a series of numerical simulations was performed using the fire dynamics simulation software (FDS) developed by the National Institute of Standards and Technology (NIST) (Kawabata N, 2003). FDS demonstrates commendable application reliability in smoke and heat transmission during tunnel fires, as evidenced by the comparison of FDS numerical simulations with experimental data (Guo et al., 2021a, b; Wang et al., 2016; Yao et al., 2021).

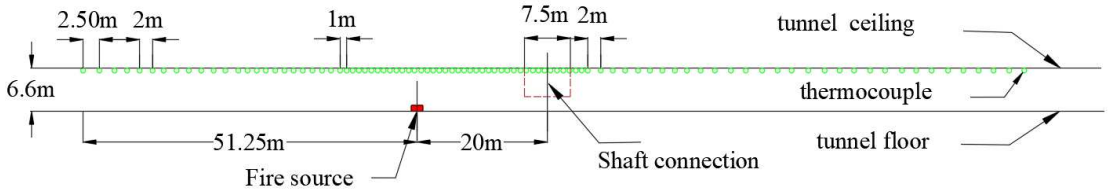
The model was created based on a survey of a tunnel in Shenzhen. It was meant to show how smoke flows in a tunnel with a lateral open shaft when there is mechanical exhaust. The computational model created in this work consists of three main parts: the main tunnel, the transverse channel, and the side opening shaft, as shown in Fig. 1(a). The main tunnel is 165 m long (L), 12 m wide (W), and 6.6 m high (H). The transverse channel, which was 12 m (L) × 7.5 m (W) × 4.2 m (H), was 71.25 m from the left port of the tunnel. The terminus of the transverse channel has a square cross-section shaft that is 56.25 m^2 in area and 42 m high. The fire source was 20 m away from the canal that went across. Five Heat Release Rates (HRR) were selected to simulate fire scenarios for different vehicle categories: 3 MW, 5 MW, 10 MW, 15

MW, and 20 MW. The temperature and pressure of the air were set at 20 °C and 1.013 kPa, respectively.

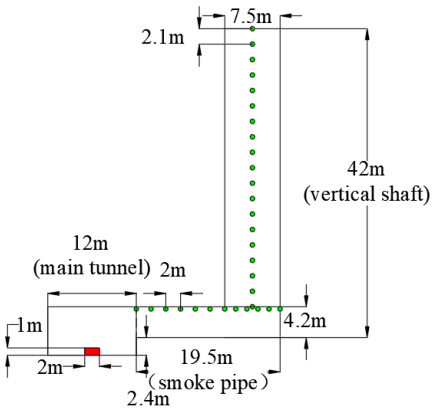
Fig. 1 (b) and (c) illustrate the configuration of measurement points within the model, encompassing the primary tunnel, the lateral smoke extraction channel, and the shaft. The thermocouple spacing in the primary tunnel at the fire source and shaft opening was established at 1 meter, while the distal spacings were set at 2 m and 2.5 m, respectively. The distance between the measurement stations in the transverse channel was 2 m. Eighteen measuring locations were established in the shaft at intervals of 2.1 m.



(a) Tunnel model stereogram



(b) Tunnel model front view



(c) Left view of the tunnel model

Fig. 1 Schematic diagram of the tunnel model

The reliability of the simulation outcome is contingent upon the selection of the appropriate grid size. The grid size δ_x is associated with the characteristic diameter of the fire source, according to the FDS user's manual (Kawabata N, 2003). A suggestion of grid size range is $16/D^*$ to $4/D^*$, as shown in Eq.(1). The characteristic diameter D^* of the fire source can be expressed as Eq.(2).

$$\frac{16}{D^*} \le \delta_x \le \frac{4}{D^*} \tag{1}$$

$$D^* = \left(\frac{\dot{Q}}{\rho_\infty c_p T_\infty \sqrt{g}} \right)^{2/5} \tag{2}$$

Where $\dot{Q}$ is the total heat release rate, ρ_∞ is air density, c_p is the specific heat capacity, T_∞ is the ambient air temperature, g is the gravity acceleration.

Grid independence analysis is an essential method for determining the appropriate grid size. Using a heat release rate of 20 MW as a reference, the equivalent diameter of the fire source is 3.09, as indicated by Eqs. (1) and (2). In order to evaluate the temperature distribution beneath the ceiling, four grid dimensions were selected to evaluate the grid's rationality. The temperature beneath the ceiling experiences a substantial decrease as the grid decreases, as illustrated in Figure 2. The temperature

beneath the ceiling remains essentially unchanged as the grid decreases from 0.25 m to 0.2 m. Nevertheless, the simulation calculations will be burdened by a smaller grid size. As a result, it is advisable to establish a grid size of 0.25 m in such situation.

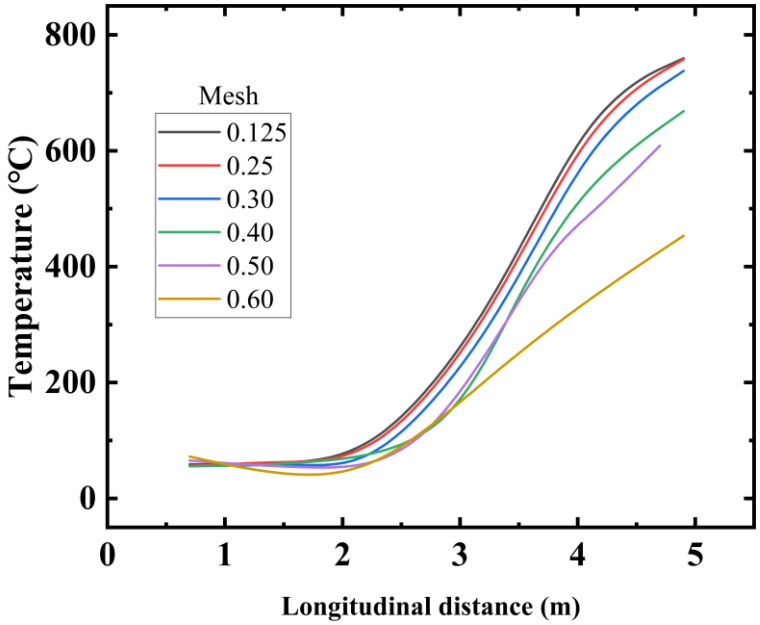


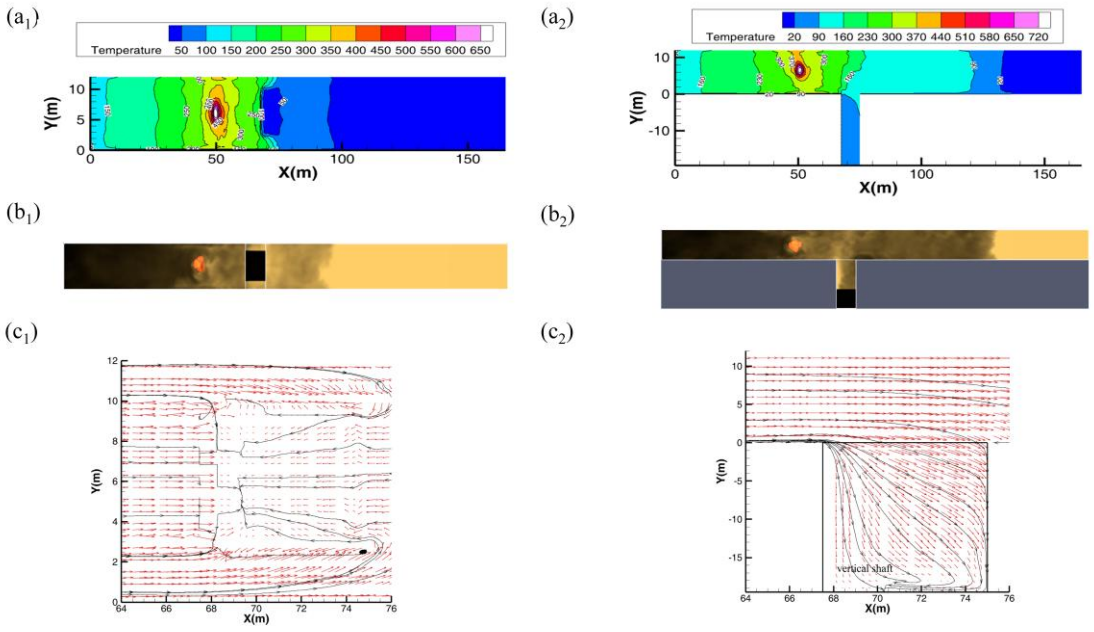
Fig.2 The temperature distribution below the ceiling under different grid settings (Q = 20 MW)

3 Results and Discussion

3.1 Effect of Mechanical smoke exhaust of side opening shaft on smoke temperature profile characteristics

To facilitate comparison, identical geometric characteristics of the shaft were chosen to replicate the fire scenario under the centralized smoke exhaust within the shaft. Fig.3 illustrates the comparative impact of lateral opening shafts and ceiling opening shafts on the parameters of smoke circulation. When the shaft opening is vertically aligned with the tunnel ceiling, the smoke trajectory exhibits axisymmetric behavior along the tunnel centerline, as evidenced by the temperature profile, smoke movement, and smoke velocity direction depicted in Fig. 3(a). However, when the vertical shaft is

linked to the main tunnel via a transverse channel, the behavior of smoke transport differs significantly from that observed with ceiling smoke extraction. An asymmetric temperature profile within the main tunnel is illustrated in Fig. 3 (b_1). The temperature gradient near the shaft side is significantly greater than that away from it, due to the considerably higher turbulent kinetic energy in proximity to the shaft. The phenomenon of boundary layer separation occurs when the downstream smoke enters the horizontal channel. As illustrated in Fig. 3 (b_3), the smoke within the transverse channel shifts towards the right side. In this scenario, smoke gathers on the right side of the horizontal channel (Fig. 3 (b_2)), leading to a comparatively elevated temperature on that side (Fig. 3 (b_1)). Furthermore, for a specified heat release rate and mechanical smoke exhaust velocity, the expense of mechanical smoke exhaust in a side opening shaft may exceed that of centralized smoke exhaust in the shaft ceiling regarding smoke management. In tunnels, the mechanical smoke exhaust system must surmount increased resistance caused by horizontal passages. Consequently, there is an increased temperature and smoke back-layering length for a mountain tunnel with a lateral open shaft.



178 Fig.3 Comparison of the effect of lateral opening shaft and ceiling opening shaft on
179 smoke movement characteristics, (a) temperature profile, (b) top view of smoke
180 movement, (c) smoke movement velocity direction, subscript 1 represents the ceiling
181 centralized smoke exhaust, and subscript 2 denotes the lateral opening shaft
182 centralized smoke exhaust.

183 The distribution of smoke temperature fields within the tunnel near the cross passage
184 and the shaft is illustrated in Fig. 4, which is characterized by varying heat release
185 rates and mechanical smoke exhaust velocities. In general, the size of the
186 high-temperature region increases as the heat discharge rate increases. The wind
187 speed increases, and the elevated temperature area decreases. It is also evident that the
188 high-temperature region in the transverse channel is consistently biased toward one
189 side, while the opposite side is the low-temperature region. In this scenario, it is
190 possible to infer that a boundary layer separation phenomenon (Fan et al., 2013; Guo
191 et al., 2021a; Ji, 2012; Jiang et al., 2020) transpires. The smoke is isolated from the

192 sidewall within the cross passage, which is referred to as the boundary layer
193 separation. This separation results in the horizontal inertial force of the smoke
194 surpassing the stack effect. Furthermore, the high temperature region is concentrated
195 on the left side of the transverse channel when the combustion intensity is low and the
196 mechanical smoke exhaust velocity is high (e.g., Fig. 4 (b) and (c)). The transverse
197 channel receives an increased volume of air from the tunnel on the right side of the
198 shaft as a result of the substantial accumulation of smoke in the tunnel on the left side
199 of the shaft. Conversely, the high temperature region is concentrated on the right side
200 of the transverse channel when the combustion intensity is high and the mechanical
201 smoke exhaust velocity is low. The smoke movement behavior will be influenced by
202 the aforementioned two competitive impacts. This could lead to a variation in the
203 nature of the smoke temperature degradation. The quantified temperature decay
204 behavior will be investigated later.

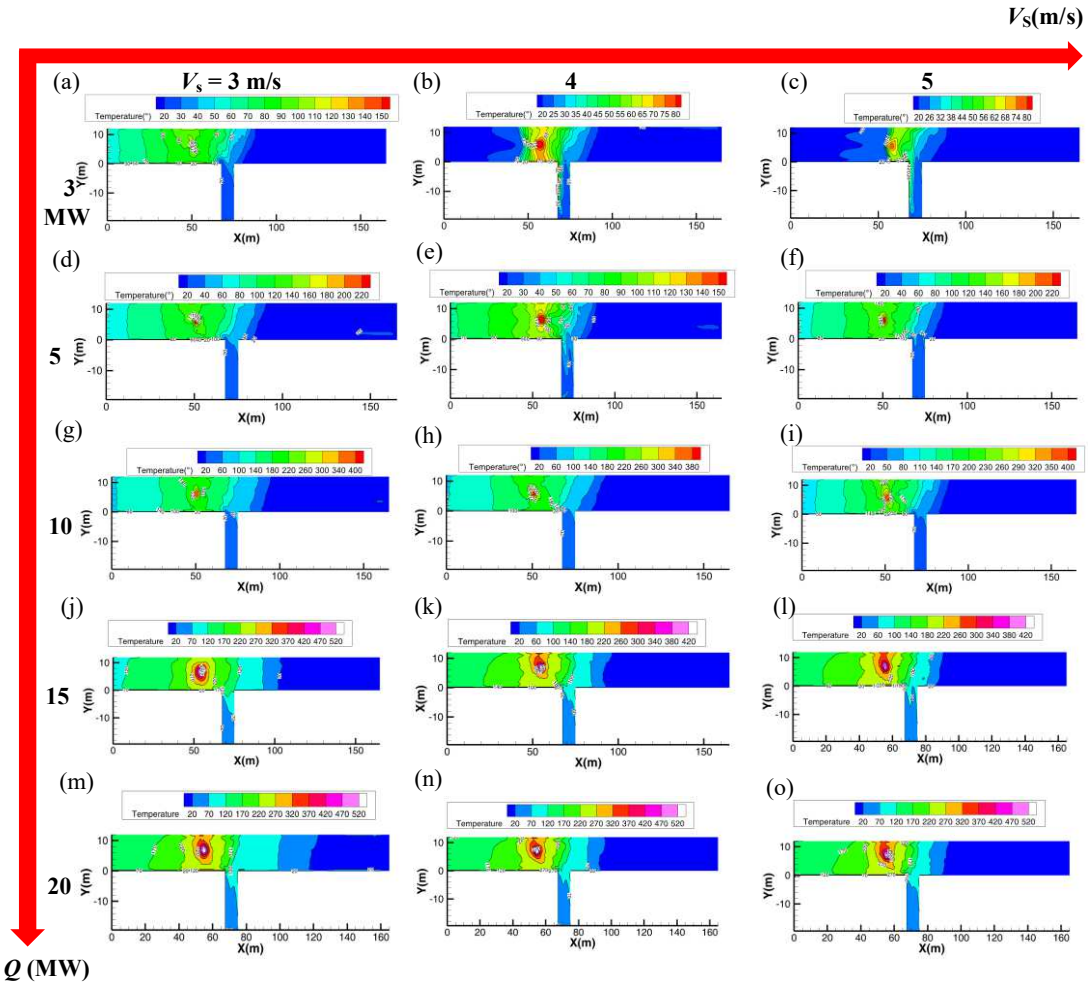


Fig.4 Smoke temperature field distribution with different mechanical smoke exhaust velocities and heat release rates.

3.2 Effect of the mechanical smoke exhaust of side opening shaft on the smoke temperature distribution

The smoke temperature distribution along the tunnel ceiling is depicted in Fig. 5 under varying mechanical smoke exhaust velocities and heat release rates. It is evident that the temperature beneath the ceiling rises in tandem with the rate of heat release. The reason for this is that the combustion intensity increases as the heat release rate increases (Alpert, 1975; Karlsson and Quintiere, 1999; Li et al., 2025b). The temperature beneath the ceiling experiences a substantial decrease as the

mechanical smoke exhaust velocity increases. Additionally, the smoke migration distance decreases as the mechanical smoke exhaust velocity increases. This suggests that the longitudinal smoke temperature degradation rate will fluctuate in accordance with the mechanical smoke exhaust velocity. Therefore, it is imperative to clarify the impact of mechanical exhaust velocity and heat release rate on the behavior of smoke temperature attenuation prior to the development of the longitudinal smoke temperature attenuation prediction model. Subsequently, this information will be examined.

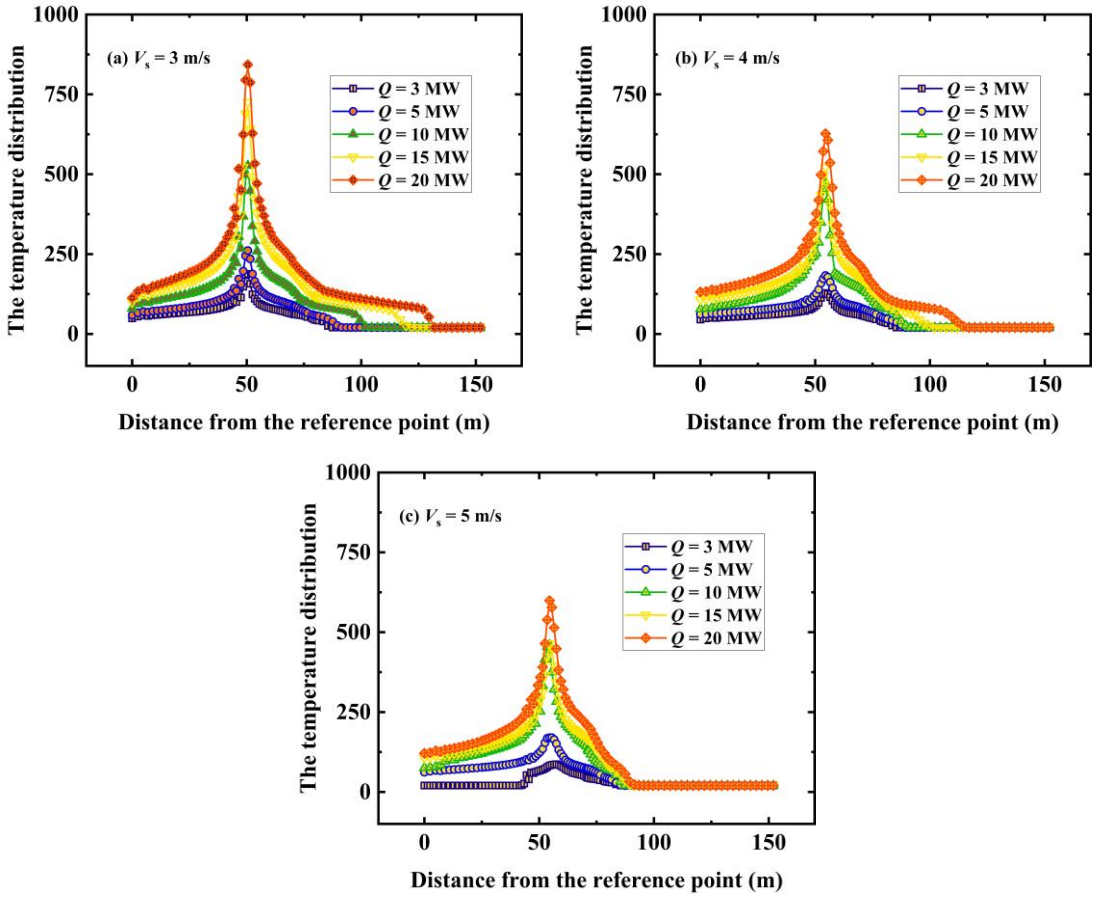


Fig.5 Longitudinal temperature distribution along the tunnel ceiling

As discussed above, longitudinal smoke temperature distribution is associated with the heat release rate and the mechanical smoke exhaust velocity. Thus, it can be

227 expressed as follows:

$$\Delta T_x = f\left(Q, V_S\right) \tag{3}$$

228 Where ΔT_x is the longitudinal smoke temperature excess.

229 As we are all aware, the longitudinal smoke temperature in tunnel fires is a function
230 of the longitudinal distance in an exponential fashion (Hu et al., 2004; Ji et al., 2012;
231 Li et al., 2021a; Li et al., 2024; Luan et al., 2021; Peng et al., 2020; Tang et al., 2017a).
232 Nevertheless, the effect of mechanical smoke exhaust in a lateral open shaft on the
233 longitudinal smoke temperature under varying vehicle fire scales needs to be
234 discussed and analyzed. Additionally, there is a paucity of quantitative
235 characterization regarding the impact of mechanical smoke exhaust on the attenuation
236 rate. This will be one of the objectives of the subsequent activity. The behavior of
237 longitudinal smoke temperature decay is presumed to be as illustrated in Eq. (4).

$$\frac{\Delta T_x}{\Delta T_{max}} = Ae^{-x/t} + y_0 \tag{4}$$

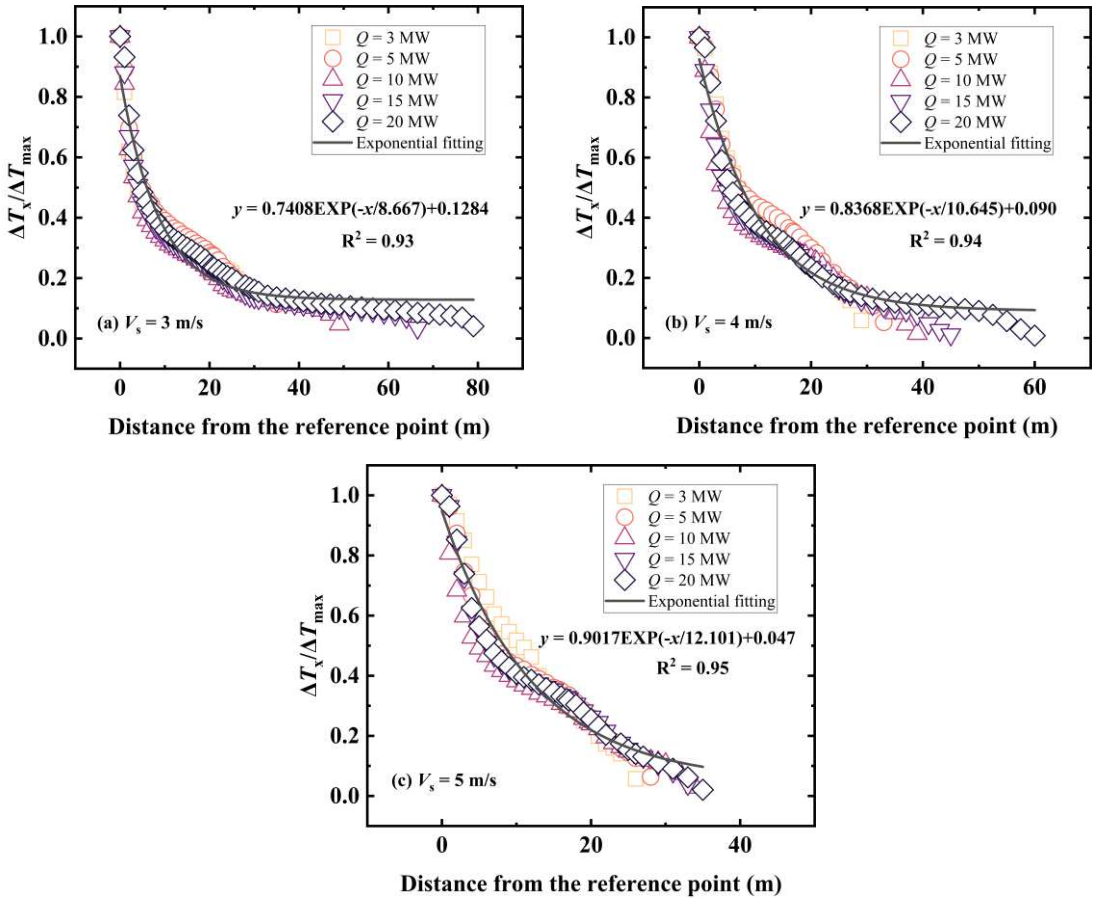
238 Where A, t and y_0 are the decay coefficients, which are associated with the heat
239 release rate and the mechanical smoke exhaust velocity.

240 Fig.6 shows the dimensionless longitudinal temperature distribution upstream with
241 different working conditions. It can be seen that the dimensionless longitudinal
242 temperature shows a small change under different heat release rates. Thus, the effect
243 of heat release rate on the longitudinal temperature decay can be ignored under
244 mechanical smoke exhaust of the side opening shaft. This situation indicates that the
245 temperature attenuation behavior of longitudinal smoke is mainly dominated by the
246 exhaust wind speed when the mechanical smoke exhaust velocity is low. In this study,

247 the mechanical smoke exhaust velocity range is from 3 m/s to 5 m/s. According to
248 fluid mechanics, the longitudinal wind speed along the shaft direction will be formed
249 in the tunnel on both sides of the shaft when the shaft mechanical ventilation system
250 is opened. A proportional relationship between the longitudinal wind speed and the
251 mechanical smoke exhaust velocity, i.e., $V_s S \propto V_{in} S_t$, was proposed previously (Han
252 et al., 2022; Hu et al., 2014), which was also verified by Zhang et al. (Zhang, 2025)
253 using experimental methods. This indicates that the induced longitudinal velocity
254 inside the tunnel is less than 1.19 m/s in this work.
255 The dimensionless mechanical exhaust velocity was implemented to quantify the
256 longitudinal smoke temperature decay behavior. The decay coefficient is illustrated in
257 Fig. 7 as a function of the dimensionless mechanical exhaust velocity. It is evident
258 that the dimensionless mechanical exhaust velocity is linearly related to all of the
259 attenuation coefficients. The dimensionless mechanical exhaust velocity is positively
260 correlated with the coefficients A and t, whereas the coefficient y_0 is negatively
261 correlated with the same. According to the gradient of coefficient with the
262 dimensionless mechanical exhaust velocity, the order of importance affecting the
263 longitudinal smoke temperature attenuation coefficient is as follows: $t > A > y_0$. The
264 correlation of the decay coefficients can be expressed as follows:
265 $y_0 = 0.647V_s^{'} + 0.504$ with the best fitting of 0.98 (R^2), $A = -0.325V_s^{'} + 0.25$ with the
266 best fitting of 0.97 (R^2), and $t = 13.811V_s^{'} + 3.601$ with the best fitting of 0.99 (R^2).
267 Consequently, the empirical model of longitudinal smoke temperature distribution
268 along the tunnel ceiling can be obtained, which can be written as follows:

$$\frac{\Delta T_x}{\Delta T_{max}} = \left(-0.325V_s^{'} + 0.25\right)e^{-x/\left(13.811V_s^{'}+3.601\right)} + 0.647V_s^{'} + 0.504 \quad (4)$$

269



270 Fig.6 Dimensionless longitudinal temperature with different smoke exhaust velocities

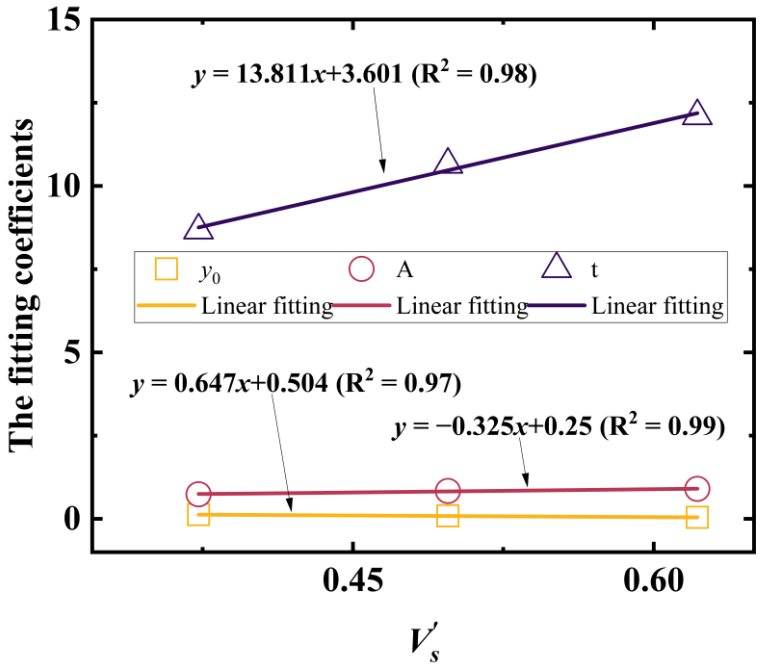


Fig.7 The fitting coefficients versus the dimensionless mechanical smoke exhaust velocity

3.3 Smoke back-layering length

The length of smoke back-layering is a crucial component in the disaster avoidance design of tunnel engineering. The instantaneous image of the fire plume inside the tunnel under mechanical smoke exhaust is plotted in Fig.8. It can be seen that more and more smoke accumulates under the ceiling, with the increase of heat release rate. In this situation, the thickness of the smoke layer increases, and the distance the smoke spreads is farther. The smoke on the downstream side of the fire source is regulated at a specific distance, from the point above the fire source to the smoke front, by the mechanical smoke exhaust. Fig.9 illustrates the length of smoke back-layering under various situations. The smoke back-layering length is markedly diminished as mechanical velocity increases. As the wind speed of the mechanical smoke exhaust in the shaft increases, the dynamic pressure generated in the tunnel

rises, resulting in more resistance to the countercurrent smoke. According to prior findings, an increase in the longitudinal wind speed of the tunnel correlates with a reduction in the velocity of the smoke front, which also elucidates the diminished length of the smoke countercurrent. Moreover, as the heat release rate escalates, the length of the smoke back-layering exhibits a notable upward tendency. The buoyancy-driven ceiling jet subsequently disperses radially; thus, the thermal buoyancy effect intensifies with an increase in the heat release rate. A quantitative investigation of the smoke back-layering length will be performed below.

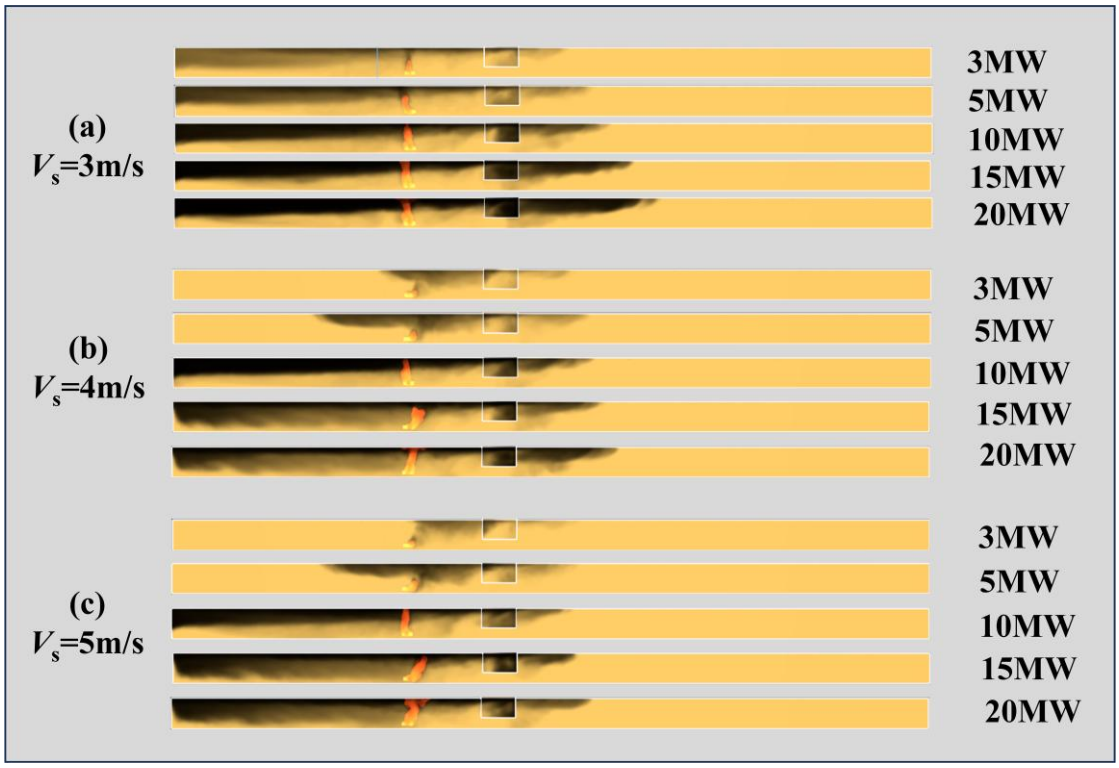


Fig.8 Instantaneous image of fire plume inside the tunnel under mechanical smoke exhaust

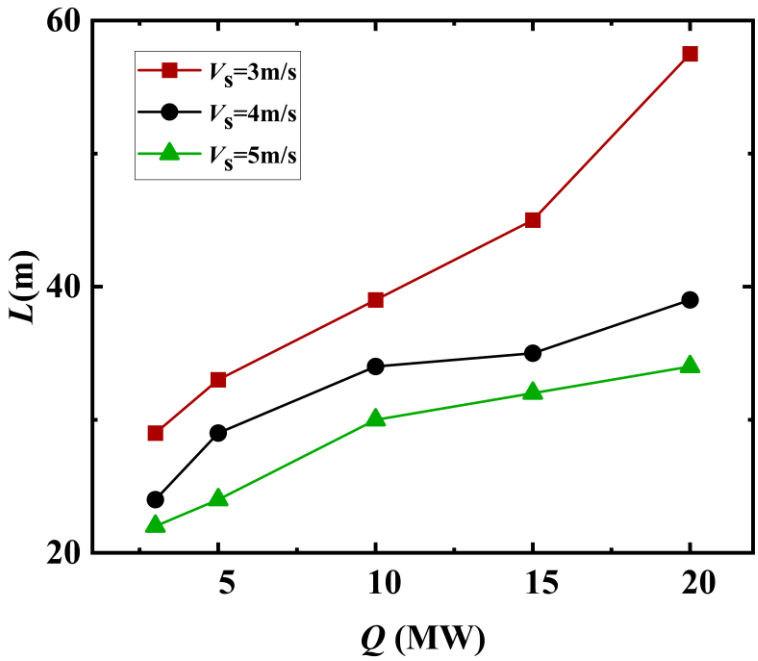


Fig.9 Smoke back-layering length with different conditions

Li et al. (Li et al., 2010) provided a model to estimate the duration of smoke back-layering, derived from a series of experiments conducted in a single-tube tunnel and dimensional analysis.

$$L^{'} = \begin{cases} 18.5\ln\left(0.81Q^{'1/3}/V^{'}\right) \\ 18.5\ln\left(0.43/V^{'}\right) \end{cases} \tag{5}$$

Tang et al.(Tang et al., 2016) examined the smoke back-layering length influenced by the combined effects of longitudinal wind and focused smoke exhaust from the ceiling. A modified model was formulated, which can be articulated as follows:

$$L^{*} = \begin{cases} 18.5\ln\left(0.81\dot{Q}^{*1/3}/V^{*}\right) \\ 18.5\ln\left(0.43/V^{*}\right) \end{cases} \tag{6}$$

$$\dot{Q}^{*} = \frac{\dot{Q} - c_p \Delta\dot{m}\Delta T_{\max} e^{-kx}}{\rho_\infty c_p T_\infty \sqrt{g} H^{5/2}} \tag{7}$$

$$V^{*} = \frac{V + \Delta\dot{m}/2A\rho_\infty}{\sqrt{gH}} \tag{8}$$

Where L^* is the dimensionless smoke back-layering length under the synergistic effect of ceiling centralized smoke exhaust and longitudinal wind, $\Delta\dot{m}$ is the smoke mass flow rate exhausted from the shaft, $\dot{Q}^*$ is the real dimensionless heat release rate inside the tunnel, V^* is the coupled dimensionless longitudinal wind speed, k is the decay coefficient. Nevertheless, when solely the shaft smoke exhaust system is engaged, Eq. (8) needs to be modified as follows:

$$v_{in}^* = \frac{\Delta\dot{m}/2A\rho_\infty}{\sqrt{gH}} \tag{9}$$

Where v_{in}^* represents the induced dimensionless longitudinal velocity under the lateral centralized smoke exhaust. As a result, the smoke mass flow rate and the actual heat release rate were influenced. Moreover, a notable distinction exists between the concentrated smoke exhaust from the side opening shaft and that from the ceiling regarding smoke migration behavior, as previously described. Consequently, a diverse smoke back-layering length requires revision. This study primarily examines buoyancy-driven plume behavior, in which the flame does not contact the ceiling. A functional relationship was assumed as $L^{*'} = \varphi\left(\dot{Q}^{*1/3}, v_{in}^*\right)$, and the coefficient λ was induced to illustrate the effect of smoke exhaust from a side-opening shaft on the smoke back flow behavior. Subsequently, by inserting Eq. (9) into Eq. (6), the predictive correlation for smoke back-layering length under mechanical exhaust in a tunnel with a lateral open shaft is derived, as shown in Eq. (10).

$$L^{*'} = \lambda 18.5 \ln\left(0.81\dot{Q}^{*1/3} / v_{in}^*\right) \tag{10}$$

Where $L^{*'}$ represents the modified dimensionless smoke back-layering length.

Fig.10 presents the fitting relationship of the dimensionless back-layering length,

where $\ln\left(0.81\dot{Q}^{*1/3}/v_{in}^{*}\right)$ is the abscissa and $L^{*'}$ is the ordinate. As we can see that $L^{*'}$ can be well correlated with $\ln\left(0.81\dot{Q}^{*1/3}/v_{in}^{*}\right)$. Based on the fitting of the tested result, the coefficient λ can be obtained, which is 3.14. This emphasizes the influence of centralized smoke extraction from the lateral open shaft on the control of smoke backflow behavior. Consequently, the revised model of the smoke back-layering length in a tunnel with the lateral open shaft can be obtained.

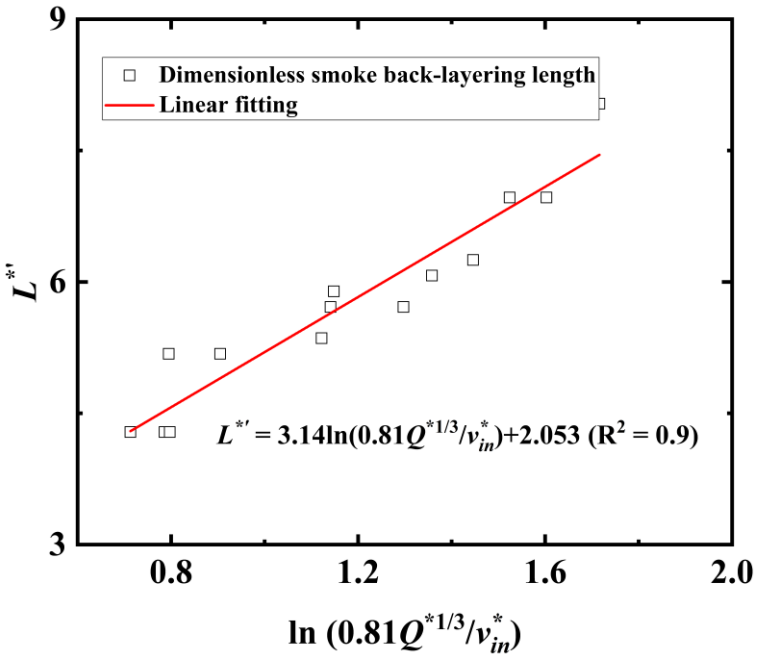


Fig.10 The relationship of the dimensionless smoke back-layering length

4. Conclusions

The fire development in a tunnel with a lateral aperture shaft was the subject of a series of numerical simulations in this work. A comparative analysis was conducted to determine the impact of the roof opening shaft and lateral opening shaft on smoke movement behavior. The effect of a mechanical smoke exhaust system with a lateral opening shaft on the temperature field distribution, longitudinal temperature decay, and smoke back-layering length was analyzed. The primary conclusions were

summarized as follows:

(1) The smoke migration behavior in the tunnel is symmetrical along the central axis of the tunnel under the mechanical smoke exhaust of the ceiling aperture shaft. Nevertheless, the temperature gradient near the shaft side is substantially higher than that away from it when the vertical shaft is connected to the main tunnel via a transverse channel.

(2) The temperature distribution beneath the ceiling diminishes progressively with an increase in the exhaust velocity of the side opening shaft. The influence of heat release rate on the decay rate of upstream smoke can be largely disregarded. The impact of mechanical smoke exhaust velocity on longitudinal temperature decay is assessed by introducing three decay coefficients, with the order of significance influencing the longitudinal smoke temperature attenuation coefficient as follows: $t > A > y_0$.

(3) The smoke back-layering length decreases as the mechanical exhaust velocity of the side aperture shaft increases. An induced velocity was implemented to quantify the impact of lateral mechanical smoke exhaust on smoke movement. Consequently, empirical correlations were proposed for the smoke back-layering length, which are suitable for the lateral centralized smoke exhaust mode in a tunnel.

Funding

This work was supported by National Natural Science Foundation of China (NSFC) under Grant No. 52508440, National Key R&D Program of China under

2023YFC2907205，2022YFC2904104. Science and Technology Project of Hebei Education Department under Grant No. QN2025304, Hebei Natural Science Foundation under Grant No. E2025402033, Handan city social science federation annual key projects under Grant No.2025483, the Innovation Fund Project of Hebei University of Engineering under Grant No. SJ2401002066.

Data Availability

All relevant data are within the manuscript.

References

Alpert, R.L., 1975. Turbulent Ceiling-Jet Induced by Large-Scale Fires. *Combustion Science and Technology* 11, 197-213.

Beard, A.N., 2009. Fire safety in tunnels. *Fire Safety J* 44, 276-278.

Chen, L.F., Hu, L.H., Tang, W., Yi, L., 2013. Studies on buoyancy driven two-directional smoke flow layering length with combination of point extraction and longitudinal ventilation in tunnel fires. *Fire Safety J* 59, 94-101.

Chen, L.F., Hu, L.H., Zhang, X.L., Zhang, X.Z., Zhang, X.C., Yang, L.Z., 2015. Thermal buoyant smoke back-layering flow length in a longitudinal ventilated tunnel with ceiling extraction at difference distance from heat source. *Appl Therm Eng* 78, 129-135.

Chow, W.K., Gao, Y., Zhao, J.H., Dang, J.F., Chow, C.L., Miao, L., 2015. Smoke movement in tilted tunnel fires with longitudinal ventilation. *Fire Safety J* 75, 14-22.

Fan, C.G., Ji, J., Gao, Z.H., Han, J.Y., Sun, J.H., 2013. Experimental study of air entrainment mode with natural ventilation using shafts in road tunnel fires. *International Journal of Heat and Mass Transfer* 56, 750-757.

Gong, L., Jiang, L., Li, S., Shen, N., Zhang, Y., Sun, J., 2016. Theoretical and experimental study on longitudinal smoke temperature distribution in tunnel fires. *Int J of Ther Sci* 102, 319-328.

Guo, Q., Li, Y.Z., Ingason, H., Yan, Z., Zhu, H., 2021a. Theoretical and numerical study on mass flow rates of smoke exhausted from short vertical shafts in naturally ventilated urban road tunnel fires. *Tunn Undergr Sp Tech* 111.

Guo, Q., Li, Y.Z., Ingason, H., Yan, Z., Zhu, H., 2021b. Theoretical studies on buoyancy-driven ceiling jets of tunnel fires with natural ventilation. *Fire Safety J* 119.

Han, J., Geng, P., Wang, Z., Lu, Y., Wang, F., Wen, J., Liu, F., 2022. Effect of ceiling extraction on the smoke spreading characteristics and temperature profiles in a tunnel with one closed end. *Tunn Undergr Sp Tech* 119.

Hu, L.H., Chen, L.F., Tang, W., 2014. A global model on temperature profile of buoyant ceiling gas flow in a channel with combining mass and heat loss due to ceiling extraction and longitudinal forced air flow. *International Journal of Heat and Mass Transfer* 79, 885-892.

Hu, L.H., Huo, R., Chow, W.K., 2008. Studies on buoyancy-driven back-layering flow in tunnel fires.

Exp Therm Fluid Sci 32, 1468-1483.
Hu, L.H., Huo, R., Chow, W.K., Wang, H.B., Yang, r.X., 2004. Decay of buoyant smoke layer temperature along the longitudinal direction in tunnel fires. *Journal of applied fire science* 13, 25.
Ingason H, L.Y.Z., Lönnermark A. , 2015. Tunnel fire dynamics. *Springer* New York.
Ji, J., Fan, C.G., Zhong, W., Shen, X.B., Sun, J.H., 2012. Experimental investigation on influence of different transverse fire locations on maximum smoke temperature under the tunnel ceiling. *International Journal of Heat and Mass Transfer* 55, 4817-4826.
Ji, J., Gao, Z. H., Fan, C. G., Zhong, W., Sun, J. H. , 2012. A study of the effect of plug-holing and boundary layer separation on natural ventilation with vertical shaft in urban road tunnel fires. *International Journal of Heat and Mass Transfer* 55, 6032-6041.
Jiang, X., Xiang, Y., Wang, Z., Mao, Y., Park, H., 2020. A numerical study on the effect of the shaft group arrangement on the natural ventilation performance in tunnel fires. *Tunn Undergr Sp Tech* 103.
Karlsson, B., Quintiere, J., 1999. Enclosure fire dynamics. *CRC press*, United States of America
Kawabata N, K.Y., Yamamoto N, Takekuni, K., & Shimoda, 2003. Numerical simulation of smoke descent in a tunnel fire. *Tunnel Management International* 4, 1-10.
Kurioka, H., Oka, Y., Satoh, H., Sugawa, O., 2003. Fire properties in near field of square fire source with longitudinal ventilation in tunnels. *Fire Safety J* 38, 319-340.
Li, Y.Z., Lei, B., Ingason, H., 2010. Study of critical velocity and backlayering length in longitudinally ventilated tunnel fires. *Fire Safety J* 45, 361-370.
Li, Y.Z., Lei, B., Ingason, H., 2011. The maximum temperature of buoyancy-driven smoke flow beneath the ceiling in tunnel fires. *Fire Safety J* 46, 204-210.
Li, Z., Gao, Y., Li, X., Mao, P., Zhang, Y., Jin, K., Li, T., Chen, L., 2021a. Effects of transverse fire locations on flame length and temperature distribution in a bifurcated tunnel fire. *Tunn Undergr Sp Tech* 112, 103893.
Li, Z., Zhang, Y., Cheng, Y., Lin, Y., Gao, Y., Luo, D., 2025a. Full-scale experimental investigation and analysis of transverse temperature profile and smoke back-layering length in an extralong mountain tunnel with ambient wind. *Process Safety and Environmental Protection* 201.
Li, Z., Zhang, Y., Gao, Y., Chen, L., Li, T., 2024. Study the maximum temperature of diffusion smoke downstream in a longitudinal ventilated branched tunnel with different transverse fire locations. *Tunn Undergr Sp Tech* 146.
Li, Z., Zhang, Y., Guo, H., Lin, Y., Cheng, Y., Gao, Y., Chen, L., Li, X., Xing, S., Li, T., 2021b. Experimental Study on the Influence of Fire Source Elevation on Smoke Temperature Profile Driven by Buoyancy in a Full-scale Mountain Tunnel. *Combustion Science and Technology* 195, 1151-1168.
Li, Z., Zhang, Y., Jiang, H., Tang, C., Luo, D., Chen, L., Lin, Y., Li, T., 2022. Effect of Fire Source Elevation on the Smoke Spreading Characteristics in an Extra-Long Tunnel. *Fire Technol* 60, 1313-1332.
Li, Z., Zhang, Y., Liu, D., Gao, Y., Chen, L., Lan, S., Hou, W., 2025b. Experimental investigation and analysis of the diffusion flames and maximum temperature characteristics of rectangular burner with weak and strong plumes in a bifurcated tunnel. *Energy* 333.
Luan, D., Yi, L., Yang, L., Chen, T., Tao, H., Xu, Z., Fan, C., 2021. Experimental investigation of smoke temperature and movement characteristics in tunnel fires with canyon cross wind. *Journal of Wind Engineering and Industrial Aerodynamics* 210.
Peng, M., Cheng, X., He, K., Cong, W., Shi, L., Yuen, R., 2020. Experimental study on ceiling smoke temperature distributions in near field of pool fires in the subway train. *Journal of Wind Engineering*

and Industrial Aerodynamics 199.
Ren, R., Zhou, H., Hu, Z., He, S., Wang, X., 2019. Statistical analysis of fire accidents in Chinese highway tunnels 2000–2016. *Tunn Undergr Sp Tech* 83, 452-460.
Tang, F., Cao, Z., He, Z., Ling, X., Wang, Q., 2018a. Thermal plume temperature profile of buoyancy-driven ceiling jet in a channel fire using ceiling smoke extraction. *Tunn Undergr Sp Tech* 78, 215-221.
Tang, F., He, Q., Mei, F., Shi, Q., Chen, L., Lu, K., 2018b. Fire-induced temperature distribution beneath ceiling and air entrainment coefficient characteristics in a tunnel with point extraction system. *Int J of Ther Sci* 134, 363-369.
Tang, F., Li, L., Chen, W., Tao, C., Zhan, Z., 2017a. Studies on ceiling maximum thermal smoke temperature and longitudinal decay in a tunnel fire with different transverse gas burner locations. *Appl Therm Eng* 110, 1674-1681.
Tang, F., Li, L.J., Mei, F.Z., Dong, M.S., 2016. Thermal smoke back-layering flow length with ceiling extraction at upstream side of fire source in a longitudinal ventilated tunnel. *Appl Therm Eng* 106, 125-130.
Tang, F., Mei, F.Z., Wang, Q., He, Z., Fan, C.G., Tao, C.F., 2017b. Maximum temperature beneath the ceiling in tunnel fires with combination of ceiling mechanical smoke extraction and longitudinal ventilation. *Tunn Undergr Sp Tech* 68, 231-237.
Wan, H., Gao, Z., Han, J., Ji, J., Ye, M., Zhang, Y., 2019. A numerical study on smoke back-layering length and inlet air velocity of fires in an inclined tunnel under natural ventilation with a vertical shaft. *Int J of Ther Sci* 138, 293-303.
Wang, J., Yuan, J., Fang, Z., Tang, Z., Qian, P., Ye, J., 2018. A model for predicting smoke back-layering length in tunnel fires with the combination of longitudinal ventilation and point extraction ventilation in the roof. *Tunn Undergr Sp Tech* 80, 16-25.
Wang, M., Guo, X., Yu, L., Zhang, Y., Tian, Y., 2021. Experimental and numerical studies on the smoke extraction strategies by longitudinal ventilation with shafts during tunnel fire. *Tunn Undergr Sp Tech* 116.
Wang, Y.F., Sun, X.F., Liu, S., Yan, P.N., Qin, T., Zhang, B., 2016. Simulation of back-layering length in tunnel fire with vertical shafts. *Appl Therm Eng* 109, 344-350.
Xu, P., Jiang, S.P., Xing, R.J., Tan, J.Q., 2018. Full-scale immersed tunnel fire experimental research on smoke flow patterns. *Tunn Undergr Sp Tech* 81, 494-505.
Yao, Y., He, K., Peng, M., Shi, L., Cheng, X., 2021. The maximum gas temperature rises beneath the ceiling in a longitudinal ventilated tunnel fire. *Tunn Undergr Sp Tech* 108.
Zhang, Y., Liu, X., Tan, R., Hou, W., Chen, L., Xing, S., Li, Z., Guo,Y., Han, X., 2025. Experimental and theoretical study on ceiling temperature distributions in mountain tunnels with lateral open shafts. *Scientific Reports* 15, 280-295.
Zhu, Y., Tang, F., Huang, Y., 2022a. Experimental study on the smoke plug-holing phenomenon and criteria in a tunnel under the lateral smoke extraction. *Tunn Undergr Sp Tech* 121.
Zhu, Y., Zhou, J., Zhang, B., Wang, H., Huang, M., 2022b. Statistical analysis of major tunnel construction accidents in China from 2010 to 2020. *Tunn Undergr Sp Tech* 124.